Analysis of Multilayer Printed Arrays by a Modular Approach Based on the Generalized Scattering Matrix

Philippe Gay-Balmaz, José A. Encinar, and Juan R. Mosig

***Abstract*—In this paper, a modular technique is used to treat infinite multilayer printed arrays with apertures and patches of irregular shapes. Each array layer is characterized by a generalized scattering matrix (GSM) from which the overall GSM of the multilayer structure is computed. The excitation of each element is modeled as a transition from the microstrip line to an aperture in the ground plane. The GSM of this transition is computed using the reciprocity theorem and spectral domain moment method. Several arrays have been analyzed by the proposed technique and the numerical results are in good agreement with other theoretical and experimental data.**

***Index Terms*—Antennas, generalized scattering matrix, microstrip arrays, multilayered media.**

I. Introduction

MANY antenna applications, like onboard systems for earth observation and communications, require very demanding specifications in bandwidth, efficiency and polarization purity. Printed antenna arrays can meet these stringent requirements and offer various other advantages due to low weight reliability and ease of manufacture. But to achieve challenging specifications, complex multilayered arrays are usually required and the existing tools for their analysis are often not efficient or accurate enough to avoid cut and try.

Large arrays are usually analyzed starting with an infinite array model [1] and introducing the finiteness of the structure through a convolution or Fourier windwing technique [2]. The same procedure may be applied to more complicated structures, like multilayered arrays with stacked patches, needed to enlarge the bandwidth [3].

All the above techniques are global, solving the array problem at once. Consequently, they become quickly prohibitive and unsuited for parametric studies, where a change in a localized parameter forces us to completely analyze again the whole structure.

We introduce here a full-wave modular approach that consists of characterizing each array layer by a generalized scattering matrix (GSM) and then analyzing the whole structure using a cascading process. This approach is very flexible for analyzing arbitrary geometries since the matrix that characterizes each layer is computed independently, and is used as a building block for the analysis of multilayer structures. Using this technique, the individual problems for each array or transition involves very simple two-layer Green functions and the number of unknowns does not increase with the number of layers. An additional layer only requires solving an additional two-layer problem and simple matrix operations for the cascade process. This modular technique has been successfully applied for the analysis of frequency selective surfaces [4], and coaxial fed [5] and cavity backed [6] printed arrays. These ideas can be directly applied to line-feed arrays if the transitions from the microstrip lines are also characterized by a GSM.

The GSM of the transition microstrip line rectangular aperture was computed in a previous work [7] and applied for the analysis of printed arrays. But the feed line was considered infinite for the GSM computation and the finite stub for the excitation of each array element is taken into account by a transmission-line model. Transmission line and equivalent circuit approaches are also at the basis of the GSM treatment of aperture coupled microstrip antennas presented in [8].

These limitations are removed in this work, where a modular approach based on the cascade of individual GSM's is applied to analyze the type of multilayer aperture-coupled printed arrays shown in Fig. 1. Also, opposite to previous works [7], [8], nonrectangular apertures are considered to improve the coupling from microstrip lines to the patches and bandwidth [9], [10]. To characterize the excitation from the microstrip line, a general three-port GSM is computed that relates the two microstrip line ports and the upper side of an array of arbitrarily shaped apertures as the third port.

The computation of the three-port GSM is described in Section II and the analysis of multilayer arrays by cascading the GSM's in Section III. To validate the proposed technique, comparisons between numerical and experimental results are shown in Section IV and, finally, a three-array stacked structure is analyzed.

II. Theory: Three-Port GSM of a Microstrip Line-Slot Transition in an Array Environment

We assume infinite array conditions, and the analysis is reduced to a single periodic cell of the array. The microstrip line-slot transition in a cell with transverse dimensions A and B, shown in Fig. 2, is considered as a basic building block. The

Manuscript received September 13, 1998; revised October 12, 1999. This work was supported in part by the Spanish 'Comisión Interministerial de la Ciencia y Tecnología (CICYT TIC98-0929-C02-01)' and by the Swiss National Science Foundation.

P. Gay-Balmaz and J. A. Encinar are with the Electromagnetism and Circuit Theory Department, Polytechnic University of Madrid, 28040 Spain.

J. R. Mosig is with the Swiss Federal Institute of Technology, Lausanne, CH—1015 Switzerland.

Publisher Item Identifier S 0018-926X(00)01275-8.

0018–9219/00$10.00 © 2000 IEEE

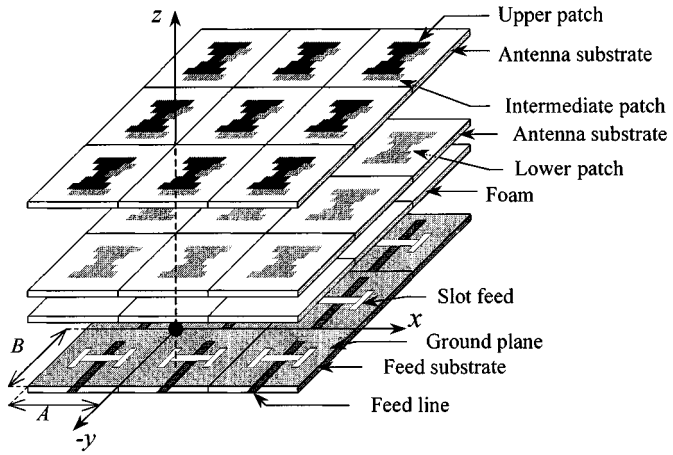

Fig. 1. Geometry of an aperture-coupled stacked-patch array.

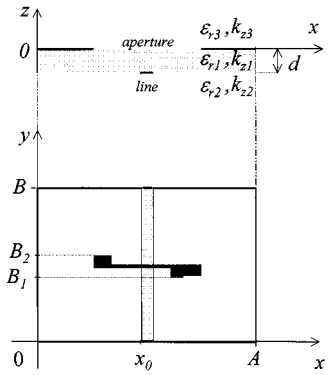

Fig. 2. Top view and vertical (xz) cut of the microstrip-slot transition in a periodic cell.

aperture is considered in an array environment and, therefore, the mutual coupling among apertures on both sides is taken into account. However, in order to simplify the analysis and to allow flexibility for the excitation of the array elements, the feed line is assumed isolated from the lines in other cells, i.e., the coupling between the feed lines themselves is neglected as is usual in microstrip lines [1]. Since we wish to find a generalized three-port description of the transition, we will consider it simultaneously excited from the two microstrip line ports and from the upper side of the slot as symbolically depicted in Fig. 3(a).

A quasi-TEM mode is assumed as the incident field at the microstrip line ports, propagating in the $\pm\hat{\mathbf{y}}$ direction with transverse modal fields given by $\mathbf{e}_m = e_{xm}\hat{\mathbf{x}} + e_{zm}\hat{\mathbf{z}}$ and $\mathbf{h}_m = h_{xm}\hat{\mathbf{x}} + h_{zm}\hat{\mathbf{z}}$, where the electric and magnetic field vectors in the microstrip $\mathbf{e}_m$ and $\mathbf{h}_m$ are normalized so that

$$\int_{z=-\infty}^{0}\int_{x=-\infty}^{+\infty} (\mathbf{e}_m \times \mathbf{h}_m)\cdot\hat{\mathbf{y}}\, dx\, dz = 1. \tag{1}$$

Assuming that the evanescent fields produced by the aperture are negligible at the two microstrip ports, the fields can be expressed as incident plus scattered fundamental quasi-TEM modes. At port 1, the fields are written as

$$\mathbf{E}_m = [d\exp(-j\beta y) + a\exp(+j\beta y)]\mathbf{e}_m$$

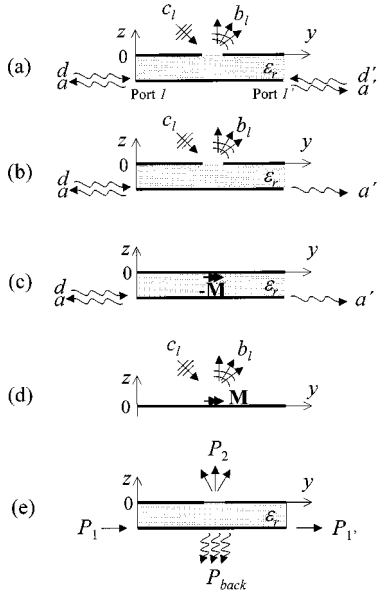

Fig. 3. Transition from microstrip to an aperture in a periodical environment. (a) Three-port representation of the transition. (b) Two-port representation with port 1′ matched. (c) Equivalent lower problem ($z < 0$). (d) Equivalent upper problem ($z > 0$). (e) Power distribution in the three-port transition: microstrip line-slot.

$$\mathbf{H}_m = [d\exp(-j\beta y) - a\exp(+j\beta y)]\mathbf{h}_m \tag{2}$$

where β is the propagation constant of the line.

Similarly, fields at port 1′ are written replacing y by B-y in (2), changing the sign of $\mathbf{H}_m$, and replacing the complex amplitudes a and d with a' and d'. From the upper side an arbitrarily incident field is assumed, which is expressed as a summation of TE $(1 \le l \le L)$ and TM $(L+1 \le l \le 2L)$ Floquet harmonics with amplitudes c_l. As is customary, subindex l includes all the ordered pairs (m, n) of Floquet harmonics, ordered as the cutoff frequency increases. The transverse (to z) incident electric field is written as

$$\mathbf{E}_i = \sum_{l=1}^{2L} c_l \mathbf{e}_l \exp(j(k_{xmx} + k_{yn}y + k_{zl}z)). \tag{3}$$

Similarly, the transverse scattered electric field, which is unknown, is expressed as

$$\mathbf{E}_s = \sum_{l=1}^{2L} b_l \mathbf{e}_l \exp(j(k_{xm}x + k_{yn}y - k_{zl}z)). \tag{4}$$

In these equations, the expression of the field $\mathbf{e}_l$ is given by

$$\begin{cases} \mathbf{e}_l = \dfrac{\sqrt{\dfrac{\eta_0}{AB}}}{\sqrt{k_{xm}^2 + k_{yn}^2}}(-k_{yn}\hat{\mathbf{x}} + k_{xm}\hat{\mathbf{y}}) \\ \qquad \text{for } 1 \le l \le L \\ \mathbf{e}_l = \dfrac{\sqrt{\dfrac{\eta_0}{AB}}}{\sqrt{k_{xm}^2 + k_{yn}^2}}(k_{xm}\hat{\mathbf{x}} + k_{yn}\hat{\mathbf{y}}) \\ \qquad \text{for } L+1 \le l \le 2L \end{cases} \tag{5}$$

with

$$\begin{cases} k_{xm} = k_0 \sin\theta\cos\varphi + 2n\pi/A = k_{x0} + 2m\pi/A \\ k_{yn} = k_0 \sin\theta\sin\varphi + 2n\pi/B = k_{y0} + 2n\pi/B. \end{cases}$$

$\eta_0 = \sqrt{\mu_0/\epsilon_0}$ is the intrinsic impedance of the free-space, k_0 is the free-space wavenumber, (θ, φ) the usual spherical angles characterizing the direction of the incident or radiated antenna beam that corresponds to the $l = 1$ $(m = n = 0)$ space harmonic. Using the fields normalized as in (5), the power transmitted by the l space harmonic is η_0/Z_l, where Z_l is the mode impedance.

To compute the three-port GSM of the transition relating the amplitudes of the incident and scattered modes at the three ports, we will consider different properties and conditions as described in the following subsections.

A. Definition of the Three-Port GSM for the Transition Microstrip Line Slot

By applying superposition, we need only consider the excitation from one microstrip port, assuming the other being matched, as shown in Fig. 3(b). Under these conditions, we consider a GSM that relates the quasi-TEM waves a, d at port 1 of the microstrip line, and the Floquet harmonics b_l, c_l above the aperture defined as

$$\begin{bmatrix} a \\ \mathbf{B} \end{bmatrix} = \begin{bmatrix} S_{11} & \mathbf{S}_{12} \\ \mathbf{S}_{21} & \mathbf{S}_{22} \end{bmatrix} \begin{bmatrix} d \\ \mathbf{C} \end{bmatrix}. \tag{6}$$

$\mathbf{C} = \lfloor c_l \rfloor$ and $\mathbf{B} = \lfloor b_l \rfloor$ are column matrices of dimensions $[2L \times 1]$ with coefficients defined in (3) and (4), respectively, S_{11} is the scattering parameter for the quasi-TEM at port 1 of the microstrip, $\mathbf{S}_{22}$ is a $[2L \times 2L]$ square matrix, and $\mathbf{S}_{12}$ $(\mathbf{S}_{21})$ is a row (column) matrix. Similarly, the excitation can be considered from the second port of the microstrip, denoted here as $1'$, assuming the port 1 matched and another GSM matrix would be obtained with elements $\mathbf{S}'_{11}$, $\mathbf{S}'_{12}$, $\mathbf{S}'_{21}$, and $\mathbf{S}_{22}$. From these GSM's, the three-port GSM is obtained as follows:

$$\begin{bmatrix} a \\ a' \\ \mathbf{B} \end{bmatrix} = \begin{bmatrix} S_{11} & t & \mathbf{S}_{12} \\ t & S'_{11} & \mathbf{S}'_{12} \\ \mathbf{S}_{21} & \mathbf{S}'_{21} & \mathbf{S}_{22} \end{bmatrix} \begin{bmatrix} d \\ d' \\ \mathbf{C} \end{bmatrix} \tag{7}$$

where t is the transmission coefficient for the quasi-TEM mode, assuming no incidence from the upper side $(\mathbf{C} = \mathbf{0})$. Note that if d' (or d) is equal to zero, (6) is obtained.

B. The Lower and Upper Half-Spaces

For the computation of the two-port GSM, assuming $d' = 0$, we define two auxiliary problems in the upper $(z > 0)$ and lower $(z < 0)$ half-spaces by closing the ground plane and replacing, as customary, the slot by equivalent magnetic currents [see Fig. 3(c) and (d)].

The arbitrarily shaped aperture is replaced by a magnetic current distribution on a metallic plane, with $\mathbf{M}$ on the upper side and $-\mathbf{M}$ on the feed side in order to enforce continuity of the tangential electric field. The magnetic current is expressed as a summation of x- and y-directed rectangular rooftop basis functions B_{xi} and B_{yi}, with, respectively, amplitudes α_{xi} and α_{yi} as

$$\mathbf{M} = \sum_{i=1}^{Ix} \alpha_{xi} B_{xi} \hat{\mathbf{x}} + \sum_{i=1}^{Iy} \alpha_{yi} B_{yi} \hat{\mathbf{y}}. \tag{8}$$

The electric field at the aperture is then obtained from $\mathbf{E}_{ap} = \hat{\mathbf{z}} \times \mathbf{M}$. From the upper side, an arbitrarily incident and scattered fields are assumed, expressed as a summation of Floquet harmonics given in (3) and (4). The scattered fields include both the field reflected by the metal plane and that produced by the magnetic current.

C. Reciprocity

In the lower half-space we apply reciprocity between the incident and total fields in the microstrip, as in [11], $\int_S (\mathbf{E} \times \mathbf{H}^+) \cdot d\mathbf{s} = \int_S (\mathbf{E}^+ \times \mathbf{H}) \cdot d\mathbf{s}$, where the closed surface S is composed by the two planes $y = 0$ and $y = B$, the infinite surface for the half-space $z < 0$, and the ground plane. The expressions of the incident electric and magnetic field are given by $\mathbf{E}^+ = \mathbf{e}_m \exp(-j\beta y)$ and $\mathbf{H}^+ = \mathbf{h}_m \exp(-j\beta y)$. The total field at $y = 0$ is expressed by (2) and at $y = B$ by the equations of the quasi-TEM mode propagating toward $+\mathbf{y}$ with amplitude a'. After applying reciprocity, the amplitude of the reflected mode in the microstrip line a is obtained as a function of the transverse electric field at the aperture as follows:

$$a = \tfrac{1}{2} \int_{S_{ap}} (\mathbf{E}_{ap} \times \mathbf{h}_m) \cdot \hat{\mathbf{z}} \exp(-j\beta y)\, d\mathbf{s}. \tag{9}$$

After substituting $\mathbf{E}_{ap}$ by its expression, (9) is written in matrix form

$$a = -\mathbf{P}^t \Lambda \tag{10}$$

where Λ is a column matrix containing the unknowns α_{xi} $(i = 1, I_x)$ and α_{yi} $(i = 1, I_y)$, and $\mathbf{P}^t$ is a row matrix of elements, p_{xi} and p_{yi} given by

$$p_{ti} = \tfrac{1}{2} \int_{c_i} B_n h_{tm} \exp(-j\beta y)\, dx\, dy, \qquad t = x, y \tag{11}$$

where c_i is the surface of the ith rooftop and h_{xm}, h_{ym} the magnetic field components of the quasi-TEM mode in the microstrip. The integration in (11) has been reduced to only the aperture above the line, because the fields h_{xm} and h_{ym} decrease rapidly with the distance from the line.

Using the Fourier transform as defined in [1] and expressing h_{xm} and h_{ym} as a function of Green's functions (assuming only y-directed current in the microstrip line) one can express the coefficients p_{xi} and p_{xi} as

$$p_{ti} = \frac{1}{8\pi^2} \int_{-\infty}^{\infty} \int_{-\infty}^{\infty} \tilde{B}^*_{ti} \tilde{G}^{\mathbf{HJ}}_{ty} \tilde{J}_{my}\, dk_x\, dk_y \qquad t = x, y \tag{12}$$

The sign * denotes the complex conjugate, $\tilde{J}_{my}$ is the current distribution of the microstrip quasi-TEM mode, $\tilde{B}_{x(y)i}$ and $\tilde{G}^{\mathbf{HJ}}_{x(y)y}$ are the $x(y)$ components of the basis and dyadic Green's functions expressed in the spectral domain.

Reciprocity is also applied between the total fields in the microstrip and a mode propagating toward $-\hat{\mathbf{y}}$, on the same closed surface as before [11], $\int_S(\mathbf{E}\times\mathbf{H}^-)\cdot d\mathbf{s}=\int_S(\mathbf{E}^-\times\mathbf{H})\cdot d\mathbf{s}$ resulting in

$$a'=(d+\mathbf{P}'^{t}\Lambda)\exp(-j\beta B) \tag{13}$$

where $\mathbf{P}'$ is the same as $\mathbf{P}$, but replacing B by $-$B. a' is the amplitude of the microstrip mode at $y=B$, which is generated by both the excitation from the microstrip and from the upper side. As can be seen from (7), the transmission coefficient t is directly obtained from (13) with no incidence from the upper side ($\mathbf{C}=0$), $t=a'/d$.

D. Continuity of Magnetic Field at the Aperture

From the microstrip side, the transverse magnetic field produced by the magnetic current $-\mathbf{M}$, defined in the arbitrarily shaped aperture at $z=0^-$, is given by

$$\mathbf{H}_{-\mathbf{M}}=\frac{1}{AB}\sum_{l=1}^{\infty}\tilde{\tilde{\mathbf{G}}}_d^{\mathbf{HM}}\cdot(-\tilde{\mathbf{M}})\exp(j(k_{xm}x+k_{yn}y)). \tag{14}$$

Similarly, the transverse magnetic field produced by the magnetic current $\mathbf{M}$ on the upper side of the aperture ($z=0^+$) is expressed as

$$\mathbf{H}_{\mathbf{M}}=\frac{2}{AB}\sum_{l=1}^{\infty}\tilde{\tilde{\mathbf{G}}}_h^{\mathbf{HM}}\cdot\tilde{\mathbf{M}}\exp(j(k_{xm}x+k_{yn}y)) \tag{15}$$

where $\tilde{\tilde{\mathbf{G}}}_d^{\mathbf{HM}}$ and $2\tilde{\tilde{\mathbf{G}}}_h^{\mathbf{HM}}$ are the transverse dyadic Green's functions for the feed dielectric substrate and the upper medium, respectively, in the spectral domain. The presence of the coefficient 2 is due to the use of the Green's function for a homogeneous medium by applying image theory.

The excitation field at $z=0^+$ from the upper medium is the incident and reflected field on a ground plane (without magnetic current)

$$\mathbf{H}_e=2\sum_{l=1}^{2L}c_l\mathbf{h}_i\exp(j(k_{xm}x+k_{yn}y)) \tag{16}$$

where $\mathbf{h}_l$ is the transverse magnetic field for the l TE (TM) Floquet harmonic associated with the $\mathbf{E}$-field given in (5). The condition for the transverse magnetic field is equated as

$$\mathbf{H}_e+\mathbf{H}_{\mathbf{M}}=\mathbf{H}_m+\mathbf{H}_{-\mathbf{M}}. \tag{17}$$

Substituting (2), (14)–(16) into (17) and performing a Galerkin testing procedure, we obtain the matrix equation

$$\mathbf{P}d-\mathbf{P}'a-\mathbf{Q}\mathbf{C}=\mathbf{Z}\Lambda. \tag{18}$$

In this equation, $\mathbf{Q}$ is a $[(I_x+I_y)\times 2L]$ matrix, where the element q_{kl} represents the transverse magnetic field of the l Floquet harmonic tested with the k basis function as given by

$$\begin{aligned} q_{kl}&=\tilde{B}^*_{xk}\hat{\mathbf{x}}\cdot\mathbf{h}_l, \qquad \text{for } 1\le k\le I_x\\ q_{kl}&=\tilde{B}^*_{yk}\hat{\mathbf{y}}\cdot\mathbf{h}_l, \qquad \text{for } I_x+1\le k\le I_x+I_y \end{aligned} \tag{19}$$

and $\mathbf{Z}$ is the typical impedance matrix of the method of moments

$$z_{ki}^{sr}=\frac{1}{AB}\sum_{l=1}^{\infty}\tilde{B}^k_{sk}\cdot(\tilde{G}^{\mathbf{HM}}_{d\,sr}+\frac{1}{2}\tilde{G}^{\mathbf{HM}}_{h\,sr})\cdot\tilde{B}_{ri} \tag{20}$$

where r and s represent the x and y components of basis and Green's functions as follows: if $1\le i,k\le I_x$, $r,s=x$, and if $I_x+1\le i,k\le I_x+I_y$, then $r,s=y$. (The expressions of the Green's functions are given in the Appendix.) The numerical computation of coefficients z_{ki}^{sr} is performed using several symmetries, as described in [12], to save computer time in the summations.

E. Identification of the Scattered Field

In the region $z\ge 0$, the transverse electric scattered field can be expressed as the summation of the field reflected from the ground plane included in the excitation field plus the field generated by $\mathbf{M}$

$$\begin{aligned} \mathbf{E}_s=&-\sum_{l=1}^{2L}c_l\mathbf{e}_l\exp(j(k_{xm}x+k_{yn}y-k_{zl}z))\\ &+\frac{2}{AB}\sum_{l=1}^{\infty}\tilde{\tilde{\mathbf{G}}}_h^{\mathbf{EM}}\cdot\tilde{\mathbf{M}}\\ &\cdot\exp(j(k_{xm}+k_{yn}y-k_{zl}z)). \end{aligned} \tag{21}$$

Identifying with (4) and testing in the periodic cell using the conjugate transverse electric field for the space harmonics, the following matrix equation is obtained:

$$\mathbf{B}=-\mathbf{C}+\mathbf{V}\Lambda. \tag{22}$$

In this equation, $\mathbf{V}$ is a matrix of dimensions $[2L\times(I_x+I_y)]$, where the coefficient v_{li} represent the electric field produced by the i basis function tested by the modal field of the lth space harmonic as given by

$$\begin{aligned} v_{li}&=-\frac{2}{\eta_0}\mathbf{e}_l\cdot(\tilde{\tilde{\mathbf{G}}}_h^{\mathbf{EM}}\cdot(\tilde{B}_{xi}\hat{\mathbf{x}})), \qquad \text{for } 1\le i\le I_x\\ v_{li}&=-\frac{2}{\eta_0}\mathbf{e}_l\cdot(\tilde{\tilde{\mathbf{G}}}_h^{\mathbf{EM}}\cdot(\tilde{B}_{yi}\hat{\mathbf{y}}))\\ &\qquad \text{for } I_x+1\le i\le I_x+I_y. \end{aligned} \tag{23}$$

The expressions of the Green's function are given in the Appendix.

F. Computation of the GSM

Assuming the incidence separately from the microstrip line ($\mathbf{C}=0$) and from the upper half-space ($\mathbf{D}=0$) in (10), (18), and (22) and after some algebraic manipulations, the GSM is obtained

$$\begin{aligned} S_{11}&=\frac{-\mathbf{P}^t\mathbf{Z}^{-1}\mathbf{P}}{1-\mathbf{P}^t\mathbf{Z}^{-1}\mathbf{P}'} \quad \mathbf{S}_{12}=\frac{\mathbf{P}^t\mathbf{Z}^{-1}\mathbf{Q}}{1-\mathbf{P}^t\mathbf{Z}^{-1}\mathbf{P}'}\\ \mathbf{S}_{21}&=\mathbf{V}\mathbf{Z}^{-1}(\mathbf{P}-\mathbf{P}'\mathbf{S}_{11})\\ \mathbf{S}_{22}&=-\mathbf{I}-\mathbf{V}\mathbf{Z}^{-1}(\mathbf{P}'\mathbf{S}_{12}+\mathbf{Q}). \end{aligned} \tag{24}$$

G. Transmitted Power at the Three Ports

The transmitted power at the three ports of the transition, as shown in Fig. 3(e), can be computed directly from the amplitudes of the propagating modes at each port, i.e., from the GSM parameters and the incident fields. Assuming only a normalized incident field at port 1 ($d = 1, d' = 0, \mathbf{C} = [0]$), the transmitted power at the two microstrip ports is

$$P_1 = (1 - |S_{11}|^2), \quad P_{1'} = |a'|^2. \tag{25}$$

P_1 is the power entering the periodic cell from port 1 and $P_{1'}$ the power going out of the cell along the microstrip line. To compute the amplitude a' from (13), first the amplitudes of the rooftop basis functions for the magnetic current Λ must be obtained from (18). The power radiated to the upper side through the arbitrarily shaped aperture is expressed as a function of the Floquet harmonics as follows:

$$P_2 = \eta_0 \mathrm{Re}\left[\sum_{l=1}^{2L} \frac{|b_l|^2}{Z_l}\right] \tag{26}$$

where Z_l is the modal impedance for lth harmonic. Note that only the propagating modes contribute to the power in (26). To compute the amplitudes b_l, Λ must be substituted in (22).

The power lost in a periodic cell P_{back} due to the back radiation (the radiation of the microstrip line in the $z < 0$ half-space) cannot be computed directly, but can be obtained from the conservation of power, which is equated as

$$P_{\mathrm{back}} = P_1 - P_{1'} - P_2. \tag{27}$$

III. Analysis of Multilayer Aperture-Coupled Arrays

A three-port GSM has been computed for the simple transition microstrip line-slot in an array environment, but the excitation of each element in practical arrays include a finite stub to match the active input impedance. In this section we include the effect of the finite stub by terminating the port $1'$ by a reflection coefficient ρ_L. Therefore, the amplitude of the mode incident at port $1'$ is $d' = \rho_L a'$. Introducing this relation in (7), a new GSM is obtained that characterizes the feed from port 1 to the upper side of the aperture, including the effect of the finite stub. The coefficients of this matrix are given by

$$S_{11}^{\mathbf{f}} = S_{11} + \frac{t^2 \rho_L}{1 - S'_{11}\rho_L} \quad \mathbf{S}_{12}^{\mathbf{f}} = \mathbf{S}_{12} + \frac{t\rho_L \mathbf{S}'_{12}}{1 - S'_{11}\rho_L}$$
$$\mathbf{S}_{21}^{\mathbf{f}} = \mathbf{S}_{21} + \frac{\mathbf{S}'_{21} t\rho_L}{1 - S'_{11}\rho_L} \quad \mathbf{S}_{22}^{\mathbf{f}} = \mathbf{S}_{22} + \frac{\mathbf{S}'_{21}\mathbf{S}'_{12}\rho_L}{1 - S'_{11}\rho_L}. \tag{28}$$

Note that if port $1'$ is matched, $\rho_L = 0$, this matrix coincides with that defined in (6).

For the analysis of a multilayer printed array as shown in Fig. 1, the GSM of each patch array is computed assuming arbitrarily incident fields from both sides expressed as a summation of Floquet harmonics, as described in [4], and cascaded to obtain the overall GSM of the stacked array [4]. The resulting matrix is cascaded with the GSM of the transition microstrip line-slot given by (28) and we obtain a matrix $\mathbf{S^T}$. This matrix relates the incident and reflected mode at the microstrip line with the amplitudes of the Floquet harmonics on the upper layer c_l and b_l, which represent the incident, if any, plus the scattered fields. These amplitudes give directly the near fields by substituting them in (3) and (4) and allow the computation of the active element patterns as shown in [13]. The reflection coefficient for the quasi-TEM mode at port 1 of the microstrip line S_{11}^T gives the active reflection coefficient of the infinite array and, therefore, the active input impedance. Matrix $\mathbf{S^T}$ also provides the power transmitted at port 1 and the radiated power in a cell, using (25) and (26) respectively. The back-radiated power can be obtained from the conservation of power.

The active input impedance can also be derived using a transmission-line equivalent circuit as described in [11]. In this case, the port $1'$ is assumed matched and the aperture plus the stacked patches in a periodic cell is represented from the microstrip line as a series impedance Z in a transmission line. The GSM given in (6) is used for the cascade process with the other GSM's , and a global GSM $\mathbf{S^{Tm}}$ is obtained under matching conditions. This matrix gives the input impedance and, by identification with the transmission line model, the value of Z.

IV. Results

In order to check the validity of the proposed modular technique, numerical results for several infinite printed arrays are compared with other experimental and theoretical results available in the literature and with measurements performed with a waveguide simulator in our laboratory including a multilayered array. For each array, the convergence of the numerical results has been checked by varying the number of basis functions and Floquet harmonics.

The first structure considered is the basic three-port transition in an array environment, as analyzed in the preceding theory. It consists of a I-shaped aperture, etched on the ground plane of a matched microstrip line, radiating into a S-band waveguide simulator. The periodic cell is shown in Fig. 4(a), where all dimensions are given in millimeters. The structure has been built and measured and the magnitude of the scattering parameters is compared with the theoretical predictions in Fig. 4(b). A very good agreement is observed between numerical and experimental results, particularly in reflected (S_{11}) and radiated (S_{21}) or transmitted to the waveguide simulator power. The slight discrepancies in the transmission from port 1 to $1'$ could be explained by the fact that an infinite array of apertures has been considered in the theoretical computation, while in the experimental setup, there is only one aperture from the microstrip side because only the upper half-space is inside the waveguide simulator. In this prototype, the aperture is large and mutual coupling in the microstrip region, included in the computations but not in the measurements, may not be negligible. The back-radiated power can be obtained from the conservation of power. For example, at 5 GHz the measurements indicate that the 49% of the incident power is entering at port 1, 16% is transmitted to the waveguide, 6% to the port $1'$, and 29% is the dissipated and back-radiated power. It must be noted that this structure has been designed primarily to validate the method of analysis and

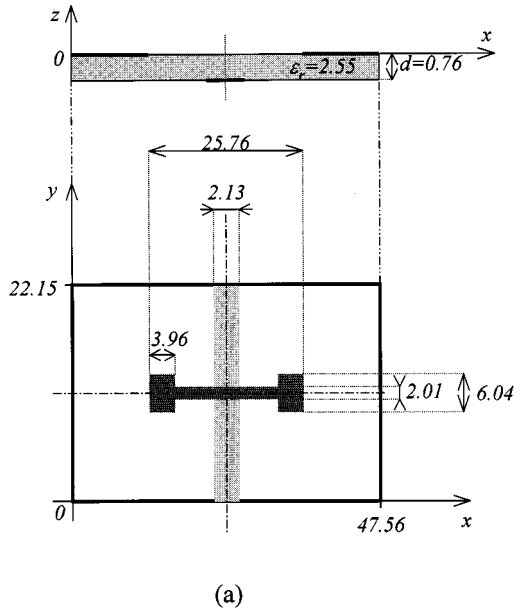

(a)

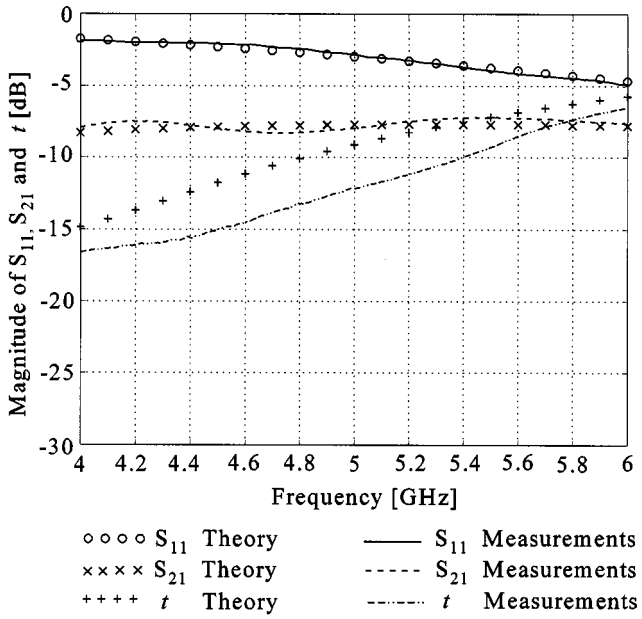

(b)

Fig. 4. Infinite array of apertures of noncanonical shape. (a) Geometry of a periodic cell. (b) Magnitude of S_{11}, t, and S_{21}. Measurements and theory.

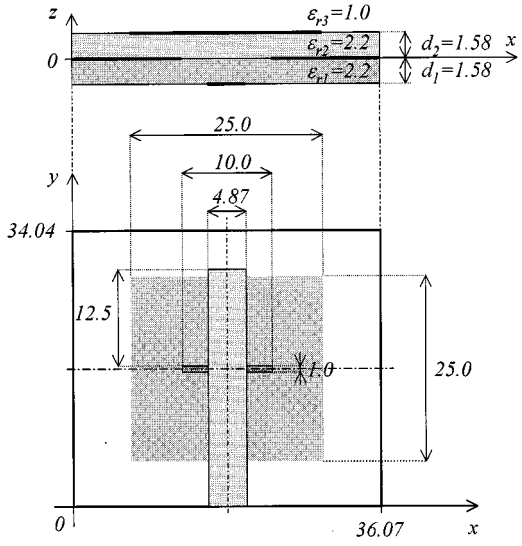

(a)

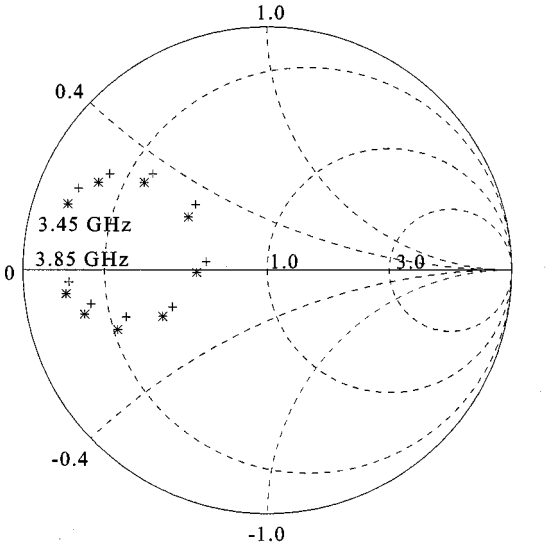

(b)

Fig. 5. (a) Dimensions and (b) active input impedance in the band 3.45–3.85 GHz for the structure presented in [1] (** theory in [1], ++ this theory).

the back-radiated power is large due to the large aperture in the ground plane.

The second structure is a one-layer printed array of aperture coupled rectangular patches previously studied by Pozar [1]. A periodic cell of this array is shown in Fig. 5(a) with all the dimensions. By means of the proposed method, the GSM of the microstrip line/slot transition is evaluated assuming port $1'$ matched. It has been checked that the input impedance obtained from $\mathbf{S^{Tm}}$ together with the transmission-line model, in this case, practically coincides with that obtained using (28). For the calculation, the periodic cell is discretized into a 36 $\times$ 34 grid and nine unknowns are used for the x-component of the magnetic current and zero for the y-component. The number of Floquet harmonics used in the cascade process is 200 (100 TM and 100 TE). The GSM of this transition is then cascaded with the GSM of the interface including the rectangular patch array. In this way, the GSM of the whole structure is found and the input impedance derived. The theoretical values for the active input impedance between 3.45 and 3.85 GHz are given in Fig. 5(b) and compared with the theoretical results of [1] with excellent agreement.

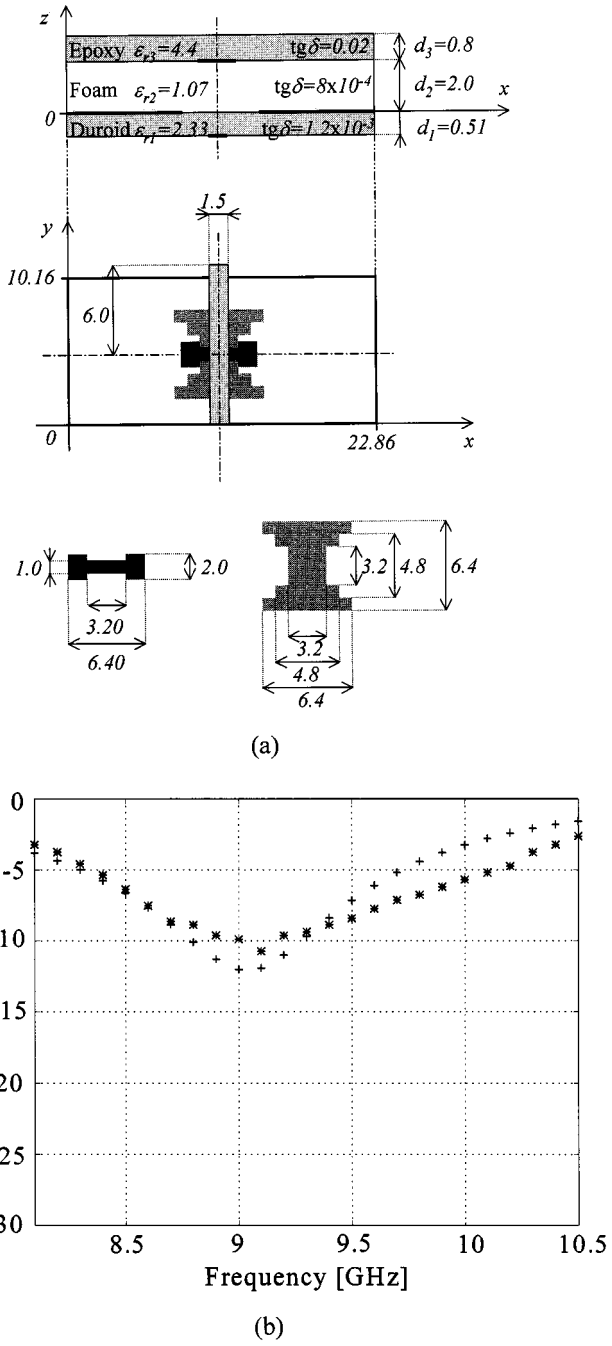

Fig. 6. Printed array measured in a waveguide simulator. (a) Geometry of a periodic cell. (b) Magnitude of the reflection coefficient from 8.1 to 10.5 GHz. (* * * measurements, + + + this theory).

Once the method has been verified, more sophisticated structures can be analyzed. For example, printed arrays with apertures and patches of noncanonical shape have been studied (see Fig. 6). The structure shown in Fig. 6(a) has been measured in a wave-guide simulator at the Swiss Federal Institute of Technology. Fig. 6(b) shows the measured and computed modules of S_{11} and demonstrates the good agreement between our theory and the measurements. The slight discrepancy could be due to the use of epoxy, an anisotropic, lossy, and badly characterized medium, as the upper substrate. A sensitivity analysis has been performed for a similar array, taking into account the tolerance of the substrate permittivities and variations of the different dimensions. The results have shown small variations in the $|S_{11}|$ and resonance frequency that also justify the discrepancies with measurements.

To prove the capabilities of the proposed method, a three-layer stacked patch array has been designed to have a very large bandwidth, built and measured with a waveguide simulator. The design was performed by analyzing the multilayer structure with only one patch array at a time, and studying its resonance separately. Then, the three patch arrays were considered simultaneously and the resonance behavior changed slightly from the individual cases. After a small adjusting of the patch dimensions, a 45% bandwidth for a VSWR $\leq$ 1.6 was obtained. The periodic cell of the array is depicted in Fig. 7(a). For the analysis, the aperture in the ground plane is modeled considering 42 x-directed and 32 y-directed magnetic currents as for the structure studied before. On each of the three patches, 36 x-directed and 32 y-directed electric currents have been used. The computer run time was 18 s per frequency on a Pentium II 400 MHz, using 100 Floquet harmonics for the cascade process. For the line-aperture transition, the computer time is 4 s and the total time increases linearly with the number of layers. The comparison between the measurements and the simulations between 3.5 and 5.75 GHz is given in Fig. 7(b) for the reflection coefficient. The measured bandwidth is 50% for a VSWR $\leq$ 1.8. In this frequency band, the radiated power (transmitted to the waveguide) is maintained between the 77% and 94% of the incident power, while the back-radiated power is less that the 16%. As for the previous prototype, a good agreement is obtained for the central frequencies and the two loops are well reproduced. The frequency shift (5%) observed experimentally can be due to fabrication tolerances or the absence of the aperture array in the prototype.

V. Conclusions

A very flexible modular technique has been proposed for the analysis of aperture-coupled stacked printed arrays, including apertures and patches of noncanonical shape. The technique is based on the computation of a GSM for each array interface, including the excitation from a microstrip line and on a later cascade process to analyze the whole multilayered structure. First, the excitation of each array element from a microstrip line through an aperture has been characterized by a GSM. The theoretical developments for the computation of the GSM of the microstrip line-slot transition have been exposed. Then, multilayered periodic structures have been analyzed by cascading iteratively the GSM of the individual interfaces considered as building blocks. Results for reflection coefficient have been presented for several arrays, showing a good agreement with other theoretical and experimental data. A broad-band array with three patch layers has been designed by using the proposed technique, built and measured in a waveguide simulator.

The proposed technique can be used to compute power at each port and the back-radiated power, the active input impedance, and the active element pattern. Also, near fields can be directly computed from the amplitudes of the Floquet harmonics above the array. This modular technique is very

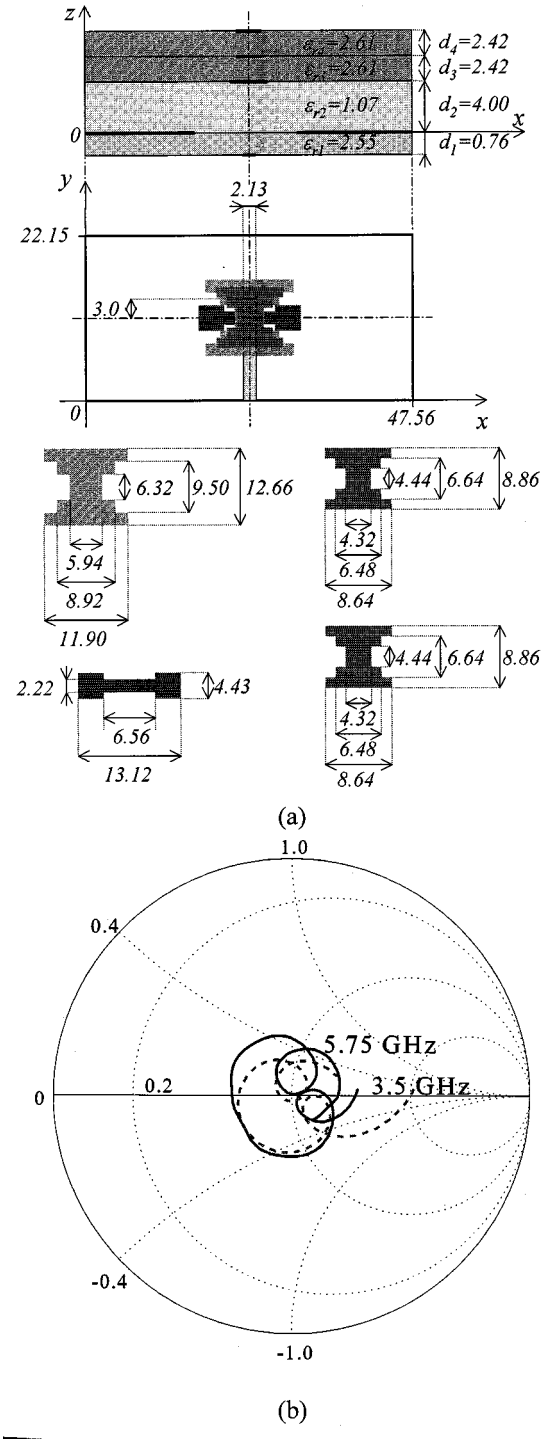

Fig. 7. Broad-band printed array, including three stacked patches of noncanonical shape in each periodic cell. (a) Geometry of a periodic cell. (b) Input impedance from 3.5 to 5.75 GHz (— measurements, - - - - theoretical results).

appropriate for parametric analyses and design procedures, since the effect of changing one parameter only affects one of the individual GSM's.

APPENDIX

This Appendix lists the required Green's functions. The wave numbers used here are defined according to Fig. 2.

Green's functions of (12)

$$\tilde{G}_{xy}^{\mathbf{HJ}} = \frac{\epsilon_{r1}k_{z1}k_{z2}\cos(k_{z1}d)+j[(k_0^2-k_y^2)\epsilon_{r1}-k_x^2]\sin(k_{z1}d)}{T_eT_m}$$

$$\tilde{G}_{yy}^{\mathbf{HJ}} = \frac{jk_xk_y(\epsilon_y(\epsilon_{r1}-1)\sin(k_{z1}d)}{T_eT_m}$$

with

$$\begin{cases} T_e = k_{z1}\cos(k_{z1}d) + jk_{z2}\sin(k_{z1}d) \\ T_m = \epsilon_{r1}k_{z2}\cos(k_{z1}d) + jk_{z1}\sin(k_{z1}d) \end{cases}$$

and

$$\begin{cases} k_{z1}^2 = \epsilon_{r1}k_0^2 - k_x^2 - k_y^2 \\ k_{z2}^2 = k_0^2 - k_x^2 - k_y^2 \end{cases}$$

where k_0 is the free-space wavenumber, d is the height of the dielectric substrate, and ϵ_{r1} its relative permittivity.

Green's function of (20)

$$\tilde{\tilde{\mathbf{G}}}_T^{\mathbf{HM}} = \tilde{\tilde{\mathbf{G}}}_d^{\mathbf{HM}} + \tfrac{1}{2}\tilde{\tilde{\mathbf{G}}}_h^{\mathbf{HM}} = \begin{pmatrix} \tilde{G}_{Txx}^{\mathbf{HM}} & \tilde{G}_{Txy}^{\mathbf{HM}} \\ \tilde{G}_{Tyx}^{\mathbf{HM}} & \tilde{G}_{Tyy}^{\mathbf{HM}} \end{pmatrix} = \begin{pmatrix} \kappa^2\tilde{G}_{Tuu}^{\mathbf{HM}} + \gamma^2\tilde{G}_{Tvv}^{\mathbf{HM}} & \gamma\kappa(\tilde{G}_{Tvv}^{\mathbf{HM}} - \tilde{G}_{Tuu}^{\mathbf{HM}} \\ \gamma\kappa(\tilde{G}_{Tvv}^{\mathbf{HM}} - \tilde{G}_{Tuu}^{\mathbf{HM}}) & \gamma^2\tilde{G}_{Tuu}^{\mathbf{HM}} + \kappa^2\tilde{G}_{Tuu}^{\mathbf{HM}} \end{pmatrix}$$

with $\gamma = (k_x/k_c)$ and $\kappa = (k_y/k_c)$, $k_c = \sqrt{k_x^2 + k_y^2}$

$$\tilde{G}_{Tuu}^{\mathbf{HM}} = \frac{-k_0}{2\eta_0}\left[\frac{\epsilon_{r3}}{k_{z3}} + \frac{\epsilon_{r1}}{k_{z1}} \cdot \frac{k_{z1}\cos(k_{z1}d) + jk_{z2}\epsilon_{r1}\sin(k_{z1}d)}{T_m}\right]$$

$$\tilde{G}_{Tvv}^{\mathbf{HM}} = \frac{-1}{2k_0\eta_0} \cdot \left[k_{z3} + \frac{k_{z1}(k_{z2}\cos(k_{z1}d) + jk_{z1}\sin(k_{z1}d))}{T_e}\right].$$

In these equations, the T_e and T_m are those defined above and $k_{z3}^2 = \epsilon_{r3}k_0^2 - k_x^2 - k_y^2$. Dyadic Green's function of (23)

$$\tilde{\tilde{\mathbf{G}}}_h^{\mathbf{EM}} = \begin{pmatrix} 0 & -1/2 \\ 1/2 & 0. \end{pmatrix}$$

The authors would like to thank Y. Brand and R.C. Hall for providing some experimental results.

REFERENCES

[1] D. M. Pozar, "Analysis of an infinite phased array of aperture coupled microstrip patches," *IEEE Trans. Antennas Propagat.*, vol. 37, pp. 418–425, Apr. 1989.

[2] A. K. Skrivervik and J. R. Mosig, "Finite phased array of microstrip patch antennas: The infinite array approach," *IEEE Trans. Antennas Propagat.*, vol. 40, pp. 579–592, May 1992.

[3] J. T. Aberle, D. M. Pozar, and J. Manges, "Phased arrays of probe-fed stacked microstrip patches," *IEEE Trans. Antennas Propagat.*, vol. 42, pp. 920–927, July 1994.

[4] C. Wan and J. A. Encinar, "Efficient computation of generalized scattering matrix for analyzing multilayered periodic structures," *IEEE Trans. Antennas Propagat.*, vol. 43, pp. 1233–1242, Oct. 1995.

[5] A. K. Bhattacharyya, "A modular approach for probe-fed capacitively coupled multilayered patch arrays," *IEEE Trans. Antennas Propagat.*, vol. 45, pp. 193–202, Feb. 1997.

[6] M. A. González, J. A. Encinar, J. Zapata, and M. Lambea, "Full wave analysis of cavity-backed and probe-fed microstrip patch arrays by a hybrid mode-matching, generalized scattering matrix and finite element method," *IEEE Trans. Antennas Propagat.*, vol. 46, pp. 234–242, Feb. 1998.
[7] J. A. Encinar, C. Wan, and J. R. Mosig, "Generalized scattering matrix computation of the transition: Microstrip line-rectangular waveguide, as a buildiing block for the analysis of multilayer microstrip circuits and antennas," in *IEEE Int. Antennas Propagat. Symp. Dig.*, Montreal, Canada, July 1997, pp. 626–629.
[8] A. K. Bhattacharyya, "A numerical model for multilayered microstrip phased-array antennas," *IEEE Trans. Antennas Propagat.*, vol. 44, pp. 1386–1393, Oct. 1996.
[9] D. M. Pozar and S. D. Targonski, "Improved coupling for aperture-coupled microstrip antenna," *Electron. Lett.*, vol. 27, pp. 1129–1131, June 20, 1991.
[10] R. C. Hall and J. R. Mosig, "The analysis of arbitrarily shaped aperture-coupled patch antennas via a mixed-potential integral equation," *IEEE Trans. Antennas Propagat.*, vol. 44, pp. 608–614, May 1996.
[11] D. M. Pozar, "A reciprocity method of analysis for printed slot and slot-coupled microstrip antennas," *IEEE Trans. Antennas Propagat.*, vol. 34, pp. 1439–1446, Dec. 1986.
[12] C. Wan and J. A. Encinar, "Exploitation of symmetries in the impedance matrix for moment-method analysis of arbitrary frequency selective surfaces," in *Proc. IEEE Antennas Propagat. Int. Symp.*, Newport Beach, CA, 1995, pp. 1648–1651.
[13] M. A. González, J. A. Encinar, and J. Zapata, "Radiation pattern computation of cavity-backed and probe-fed stacked microstrip patch arrays," IEEE Trans. Antennas Propagat., to be published.

Philippe Gay-Balmaz was born in Vernayaz, Switzerland. In 1990, he received the E.E. degree from the Ecole Polytechnique Fédérale de Lausanne (EPFL), Switzerland, and the Ph.D. degree from the Laboratory of Electromagnetics and Acoustics, EPFL, in 1996, where his thesis dealt with three-dimensional planar structures in stratified media.

From 1990 to 1996, he was a Research Associate at Laboratory of Electromagnetics and Acoustics of the EPFL, where he worked on novel printed antennas. From 1997 to 1999 he joined the Electromagnetism and Circuit Theory Department, Universidad Politécnica de Madrid (UPM), Spain. He is currently working at the Laboratory for Electromagnetic Fields and Microwave Electronics at the Swiss Federal Institute of Technology, Zurich (ETHZ). His interests include investigating multilayer printed antennas and arrays, computational electrodynamics, and nano-optics.

José A. Encinar was born in Madrid, Spain. He received the E.E. and Ph.D. degrees, both from Universidad Politécnica de Madrid (UPM), Spain, in 1979 and 1985, respectively.

Since January 1980, he has been with the Applied Electromagnetism and Microwaves Group, UPM, as a Teaching and Research Assistant from 1980 to 1982, as an Assistant Professor from 1983 to 1986, and as Associate Professor from 1986 to 1991. From February to October of 1987 he was with the Polytechnic University, Brooklyn, NY, as a Postdoctoral Fellow of the NATO Science Program. Since 1991 he has been a Professor in the Electromagnetism and Circuit Theory Department, UPM. In 1996 he was with the Laboratory of Electromagnetics and Acoustics at Ecole Polytechnique Fédérale de Lausanne (EPFL), Switzerland, as Visiting Professor. His research interests include analytical and numerical techniques for the analysis and design of waveguide structures, frequency selective surfaces, and multilayer printed arrays.

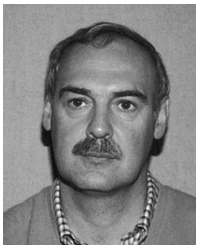

Juan R. Mosig (S'76–M'87–SM'94–F'99) was born in Cadiz, Spain. He received the E.E. degree from Universidad Politecnica de Madrid, Spain, in 1973, and the Ph.D. degree from the Laboratory of Electromagnetics and Acoustics at Ecole Polytechnique Fédérale de Lausanne (EPFL), Switzerland, in 1983.

In 1976 he joined the Laboratory of Electromagnetics and Acoustics at Ecole Polytechnique Fédérale de Lausanne (EPFL). Since 1991 he has been a Professor at EPFL. In 1984 he was a Visiting Research Associate at Rochester Institute of Technology, Rochester, NY. He has also held scientific appointments at the University of Rennes, France, the University of Nice, France, the Technical University of Denmark, and the University of Colorado at Boulder. He is the author of four chapters in books on microstrip antennas and circuits. He is co-organizer and lecturer of yearly short intensive courses in numerical electromagnetics (Europe and the United States). His research interests include electromagnetic theory, numerical methods, and microstrip antennas.

Dr. Mosig is a member of the Swiss Federal Commission for Space Applications and the responsible of several research projects for the European Space Agency.